

# Self-Organizing Materials with Low Surface Energy: The Synthesis and Solid-State Properties of Semifluorinated Side-Chain Ionenenes

Jianguo Wang and Christopher K. Ober\*

Department of Materials Science and Engineering, Cornell University, Bard Hall, Ithaca, New York 14853-1501

Received January 24, 1997; Revised Manuscript Received August 13, 1997<sup>®</sup>

**ABSTRACT:** The synthesis of new semifluorinated alkyl side-chain ionenes (SFASI) is reported and involves reaction of semifluorinated 1-bromoalkanes with poly(*N,N'*-dimethyl-1,6-hexanediamine) (PDHD) which was prepared by reduction of poly(*N,N'*-dimethylhexamethylenedipamide). The quaternization efficiency of the polyamine is 80–85% when carried out using a solvent mixture of DMF/ethanol (1/2 volume ratio) at 65 °C over long reaction times. The structure of SFASI consists of a 10 Å charged layer resulting from quaternary ammonium groups with strong coulombic interactions and a smectic B-like packing of the semifluorinated side-chain layer. The perfluorocarbon segments favor self-organization in a hexagonal array to form a head-to-head bilayer between the charged layers. These ionenes exhibit a smectic to isotropic transition, with the transition temperature dominated by the length of the fluorocarbon side chain. The surface energy of a spin-coated SFASI film, as estimated from the critical surface tension, was as low as 8 dyn/cm at 20 °C. This result indicates that the surface of the as-spun cast film consists largely of CF<sub>3</sub> end groups even though hydrophilic ammonium groups are present in the polymer. The surface segregation and orientation of the low surface energy mesogenic semifluorinated side groups were confirmed by X-ray photoelectron spectroscopy (XPS) and near-edge X-ray fine structure (NEXAFS) analysis. Surface reconstruction was observed due to polymer chain defects and surface mobility.

## Introduction

Among the various uses of fluorinated polymers, nonstick-coating materials attract great attention<sup>1–6</sup> because of their extensive use in applications such as peel-off backings for self-stick labels,<sup>7</sup> devices to prevent the accumulation of biological debris, nontoxic antifouling release coatings for ships hulls,<sup>8</sup> stain-resistant fabrics, and self-lubricating surfaces.<sup>9</sup> In general, nonstick-coating materials need a low surface energy, a function of the surface tension ( $\gamma$ ), which can be expressed by Macleod's relation<sup>10</sup>

$$\gamma = \gamma^\circ \rho^\beta \quad (1)$$

Here  $\gamma^\circ$  and  $\beta$  are constants, independent of temperature,  $\rho$  is the polymer density (which is almost constant for a given polymer), and  $\beta$  is known as Macleod's exponent and is usually 3.0–4.5 for polymers. The value  $\gamma^\circ$  is, to a close approximation, dependent only on the chemical structure of the surface. It is well-known that the surface tension of substituent groups decreases in the order of CH<sub>2</sub> (36 dyn/cm) > CH<sub>3</sub> (30 dyn/cm) > CF<sub>2</sub> (23 dyn/cm) > CF<sub>3</sub> (15 dyn/cm).<sup>11–14</sup> Among various molecular structures, a closest-packed uniform CF<sub>3</sub> surface was found to possess the lowest surface tension. Therefore, a polymeric material that can maintain a stable, uniform CF<sub>3</sub> surface might be able to play a key role in producing nonadherent materials.

The creation of tailored surfaces by the assembly of Langmuir–Blodgett (LB) monolayers using amphiphilic molecules depends on the self-recognition behavior of molecules itself dependent on van der Waals and coulombic forces. Among reported LB films, those of perfluorocarboxylic acid<sup>15–17</sup> exhibit the lowest critical

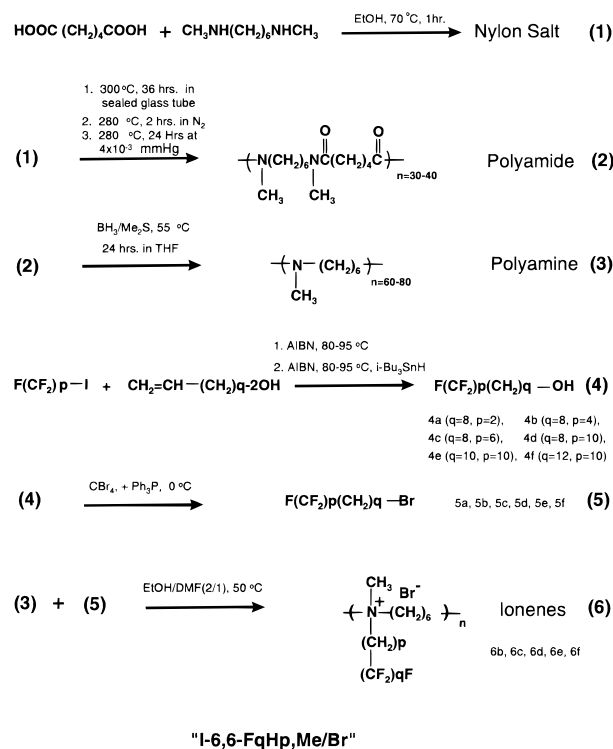
surface energy of 6–8 dyn/cm, as determined from contact angle measurements. Previous work has shown that aliphatic side chain ionenes exhibited excellent self-organization abilities,<sup>18,19</sup> in which alternating alkyl side chain and ionic layers on gold substrates could be prepared by evaporation of a polymer solution. Semifluorinated alkane diblocks<sup>20</sup> (SFAB) of even the nonpolar perfluoro-*n*-eicosane<sup>21</sup> have been shown to possess extraordinary self-assembly properties from which an ordered LB monolayer could be prepared at the air–water interface. Owing to the strong amphiphilic and liquid-crystalline character of the semifluorinated alkyl side chains, it is expected that they should possess self-assembly abilities superior to aliphatic groups in side-chain ionenes. Driven by the migration of the low surface energy –CF<sub>3</sub> ends of the semifluorinated chain to the surface, the –CF<sub>3</sub> end groups may be self-oriented at the surface to produce a low surface energy material.

Self-assembly also occurs in block copolymers due to the differing thermodynamic interactions between two or more blocks.<sup>22,23</sup> In fact, the semifluorinated alkyl chain is a miniblock oligomer because the perfluorocarbon segment ((CF<sub>2</sub>)<sub>*n*</sub>, *n* > 8) is strongly immiscible with its hydrocarbon segments.<sup>24</sup> Formation of low-energy surfaces from fluorinated block copolymers including their segregation behavior kinetics was recently discussed in detail.<sup>25,26</sup> As reported from our recent studies on the semifluorinated side-chain liquid-crystalline block copolymers,<sup>27</sup> the stability of the surface can be enhanced by the enthalpy penalty to disorder the highly ordered liquid-crystal structure of the semifluorinated compounds.

From the standpoint of molecular design, semifluorinated side-chain ionenes incorporate a number of novel features. The structure is shown in Scheme 1 and consists of a semifluorinated alkyl side chain directly connected to a quaternary ammonium backbone by a covalent bond. The goal of this research was to attempt the construction of a low surface energy material which

<sup>®</sup> Abstract published in *Advance ACS Abstracts*, October 15, 1997.

### Scheme 1. Synthesis of Semifluorinated Side-Chain Ionenes



spontaneously forms a uniform  $-\text{CF}_3$  surface. Unlike the general synthetic procedure for side-chain ionenes (*i.e.*, reaction of a side-chain diamine with dihaloalkanes<sup>28</sup>), this paper describes a more flexible pathway to introduce selected side groups during ionene synthesis *via* direct quaternization of a polyamine with haloalkanes.

We should mention that our strategy of using a highly hydrophilic backbone in a low surface energy (hydrophobic) material does not conflict with our stated goal because the quaternary ammonium group can be used as an attachment site for polar substrates by simple charge interaction or exchange of counterions. For example, Antonietti et al. also reported recently that a perfluorinated surfactant/polyelectrolyte complex possesses very low surface energy.<sup>29</sup>

### Experimental Section

**Materials.** Adipic acid (99+%), adipoyl chloride (99%), *N,N'*-dimethyl-1,6-hexanediamine (98%), 3-buten-1-ol (99%), 4-buten-1-ol (99%), 5-hexen-1-ol (99%), 9-decen-1-ol (98%), 2.0 M borane/dimethyl sulfide in tetrahydrofuran, tributyltin hydride, carbon tetrabromide (99%), and triphenylphosphine (99%) were used as received from Aldrich. Azobisisobutyronitrile (AIBN, Merck) was recrystallized from acetone/methanol (1:1) at  $0^\circ\text{C}$  after cooling down from  $40^\circ\text{C}$ . Perfluorooctyl iodide (97% minimum), perfluorodecyl iodide, perfluorododecyl iodide, and 1*H*,1*H*,2*H*,2*H*-perfluorodecane (97% minimum) purchased from PCR Inc. (Gainesville, FL) were used without any further purification.

The general procedure for synthesis of semifluorinated side-chain ionenes is shown in Scheme 1, in which the poly(*N,N'*-dimethylhexamethyleneadipamide) was prepared by high-temperature polycondensation. After homogeneous reduction, the polyamide was converted to poly(*N,N'*-dimethylhexanediamine). The polyamine was directly quaternized with semifluorinated 1-bromoalkanes which were synthesized by a functional transformation of the anti-Markov radical addition products of 1-iodoperfluorocarbon with  $\omega$ -alken-1-ol.

**Synthesis of Poly(*N,N'*-dimethylhexamethyleneadipamide) (2).** It was found that interfacial, solution, and

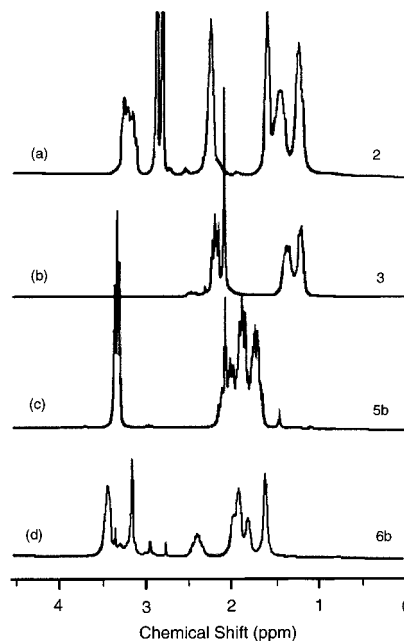


**Figure 1.**  $^1\text{H}$  NMR spectra of (a) poly(*N,N'*-dimethylhexamethyleneadipamide), (b) poly(*N*-methylhexanediamine), (c)  $\text{F}(\text{CF}_2)_8\text{-CH}_2\text{CH}_2\text{CH}_2\text{CH}_2\text{Br}$ , and (d) ionene, I-6,6-F8H4,Me/Br.

dispersion polycondensation of adipoyl chloride and *N,N'*-dimethyl-1,6-hexanediamine are difficult to use successfully because of the low reactivity of monomer and good solubility of the *N*-methyl aliphatic polyamide (2) in organic solvents. However, it is possible to synthesize the polyamide<sup>30</sup> using classical high-temperature condensation of nylon salts under strict conditions.

Portions of 0.1 mol adipic acid were slowly added to a stirring mixture of 40 mL of absolute ethanol and 0.1 mol *N,N'*-dimethyl-1,6-hexanediamine at  $60^\circ\text{C}$ , and then the reaction was raised to  $80^\circ\text{C}$  for 1 h. Crude nylon salt was obtained by rotoevaporation of the ethanol, and the crystallized nylon salt was prepared by recrystallization in a small amount of ethanol (10 mL) twice followed by drying in a vacuum oven at room temperature.

A total of 8 g of nylon salt was added to a long Pyrex glass tube, and the air was exchanged with nitrogen before sealing the tube. To prevent explosion at high temperature, an alternative method is to carry out the reaction in an autoclave. Three steps were used to achieve high molecular weight polyamines. First, the sealed glass tube was buried in a sand bath and heated gradually to  $300^\circ\text{C}$  over 4 h; the reaction was kept at this temperature for another 24 h. Then the top of the glass tube was opened and purged with nitrogen to remove water at  $250^\circ\text{C}$  for 2 h. Finally, at  $250^\circ\text{C}$ , the tube was connected to a vacuum line at  $3.5 \times 10^{-3}$  mmHg for another 18 h. The slightly brown polyamide was obtained.

Analysis of 2:  $^1\text{H}$  NMR ( $\text{CDCl}_3$ ,  $\delta$  in ppm as shown in Figure 1) 2.87, 2.94 (3H,  $\text{NCH}_3$ ), 2.31 (2H,  $\text{COCH}_2$ ), 1.45 (4H,  $\text{COCH}_2\text{CH}_2$ ), 3.31 (4H,  $\text{NCH}_3\text{CH}_2$ ), 1.65 (4H,  $\text{NCH}_3\text{CH}_2\text{CH}_2$ ), 1.28 (2H,  $\text{NCH}_3\text{CH}_2\text{CH}_2\text{CH}_2$ ).

**Synthesis of Poly(*N*-methylhexanediamine) (3).** In a dry flask, equipped with a condenser topped with a nitrogen inlet and bubbler connected by a rubber septum from the top of the condenser, 5 g (39.4 mmol) of (2) was dissolved in 100 mL of anhydrous THF under nitrogen. The solution was heated in an oil bath at  $50^\circ\text{C}$  before 90 mL of a 2 M borane/dimethyl sulfide solution was directly transferred by a double-ended needle. During the reaction, a polyamine/borane complex was formed and the brown solution changed to light yellow. After 24 h, THF and dimethyl sulfide were distilled off. Then 50 mL of degassed 6 N HCl was carefully added to the polyamine solution at  $60^\circ\text{C}$  in order to destroy any excess borane. The decomposition reaction was continued until no gas was given off. The polyamine was recovered by dumping the reaction mixture into 300 mL of a 20% NaOH solution, and the gellike

product was washed with water many times until the pH was close to neutral, ca. 8–9. The product was dissolved in diethyl ether, was dried with  $\text{Na}_2\text{CO}_3$  before drying in a vacuum oven at 40 °C for 2 days, and was finally placed in the refrigerator.

**Analysis of 3:**  $^1\text{H}$  NMR ( $\text{CDCl}_3$ ,  $\delta$  in ppm) 2.16 (3H,  $\text{NCH}_3$ ), 2.27 (4H,  $\text{NCH}_2\text{CH}_2$ ), 1.49 (4H,  $\text{CH}_3\text{NCH}_2\text{CH}_2$ ), 1.26 (4H,  $\text{CH}_3\text{NCH}_2\text{CH}_2\text{CH}_2$ );  $^{13}\text{C}$  NMR ( $\text{CDCl}_3$ ,  $\delta$  in ppm) 57.75 ( $\text{CH}_3\text{NCH}_2$ ), 42.14 ( $\text{CH}_3\text{NCH}_2$ ), 27.50 ( $\text{CH}_3\text{NCH}_2\text{CH}_2\text{CH}_2$ ), 27.15 ( $\text{CH}_3\text{NCH}_2\text{CH}_2\text{CH}_2$ ).

**General Procedure for the Synthesis of  $\omega$ -Perfluoroalkylalkanols:**  $\text{F}(\text{CF}_2)_p(\text{CH}_2)_q\text{OH}$  ( $p = 8, 10, 12$ ,  $q = 4-10$ ). Compounds **4a–f** were synthesized by radical addition of perfluoroalkyl iodide with  $\omega$ -alken-1-ol and dehalogenation. The synthetic procedure is similar to that reported by Höpken et al.<sup>31</sup> The excess  $\omega$ -alken-1-ol was distilled before reduction with tributyltin hydride in order to eliminate reaction side products during dehalogenation. The purity was checked by NMR and by comparing the melting point with that from ref 31.

**General Procedure for the Synthesis of  $\omega$ -Perfluoroalkyl-1-bromoalkanes.** In a 100 mL round-bottomed flask, 4.90 g (10 mmol) of **4a** and 4.97 g (0.015 mol) of carbon tetrabromide were dissolved in a  $\text{THF}/\text{CH}_2\text{Cl}_2$  (10 mL/20 mL) solution and cooled down to –5 °C using a brine bath before 3.93 g (15 mmol) of triphenylphosphine was added in small portions over 15 min. The reaction was maintained at –5 °C for 1 h and continued at room temperature for another 6 h. During the reaction, a white precipitate of triphenylphosphine oxide was produced gradually and the solvent became slightly pink due to formation of free bromine. The solvent was rotoevaporated and the products were extracted in 10 mL of diethyl ether four times. The crude semifluorinated 1-bromoalkane was purified by reduced pressure distillation (4.41 g, yield 79%) at 40–50 °C, 0.5–1 mmHg. **5b–5d** were prepared in the same manner. **5e** and **5f** were prepared by reaction at 5–10 °C to prevent the  $\omega$ -perfluoroalkylalkan-1-ol from precipitating out. Finally, the products were purified by passing through a short silica column (12 cm) to absorb the triphenylphosphine oxide and sublimed in a 0.2 mmHg vacuum just below the melting point.

**Analysis of 5a:**  $^1\text{H}$  NMR ( $\text{CDCl}_3$ ,  $\delta$  in ppm) 3.51 (t, 2H,  $\text{CH}_2\text{Br}$ ), 2.70 (seven, 2H,  $\text{CF}_2\text{CH}_2$ );  $^{19}\text{F}$  NMR ( $\text{CDCl}_3$ ,  $\delta$  in ppm reference as  $\text{CF}_3\text{Cl}$ ) –81.4 ( $\text{CF}_3$ ), –126.6 ( $\text{CF}_3\text{CF}_2$ ), –123.2 ( $\text{CF}_3\text{CF}_2\text{CF}_2$ ), –122.3 ( $\text{CF}_3\text{CF}_2\text{CF}_2(\text{CF}_2)_3$ ), –113.9 ( $\text{CF}_2\text{CF}_2\text{CH}_2$ ), –114.7 ( $\text{CF}_2\text{CH}_2$ ); mp = 23–25 °C.

**5b:**  $^1\text{H}$  NMR ( $\text{CDCl}_3$ ,  $\delta$  in ppm) 3.42 (t, 2H,  $\text{CH}_2\text{Br}$ ), 2.09 (2H,  $\text{CF}_2\text{CH}_2$ ), 1.95 (2H,  $\text{CH}_2\text{CH}_2\text{Br}$ ), 1.81 ( $\text{CF}_2\text{CH}_2\text{CH}_2$ ). mp 32–34 °C.

**5c:**  $^1\text{H}$  NMR ( $\text{CDCl}_3$ ,  $\delta$  in ppm) 3.41 (t, 2H,  $\text{CH}_2\text{Br}$ ), 2.06 (2H,  $\text{CF}_2\text{CH}_2$ ), 1.84 (2H,  $\text{CH}_2\text{CH}_2\text{Br}$ ), 1.60 (2H,  $\text{CF}_2\text{CH}_2\text{CH}_2$ ), 1.45 (4H,  $\text{CF}_2\text{CH}_2\text{CH}_2\text{CH}_2\text{CH}_2$ ); mp 35–37 °C.

**5d:**  $^1\text{H}$  NMR ( $\text{CDCl}_3$ ,  $\delta$  in ppm) 3.40 (t, 2H,  $\text{CH}_2\text{Br}$ ), 2.06 (2H,  $\text{CF}_2\text{CH}_2$ ), 1.84 (2H,  $\text{CH}_2\text{CH}_2\text{Br}$ ), 1.60 (2H,  $\text{CF}_2\text{CH}_2\text{CH}_2$ ), 1.30 (12H,  $\text{CF}_2\text{CH}_2\text{CH}_2(\text{CH}_2)_6\text{CH}_2\text{CH}_2\text{Br}$ ); mp 41–43 °C.

**5e:**  $^1\text{H}$  NMR is the same as **5d**; mp 64–66 °C.

**5f:**  $^1\text{H}$  NMR is the same as **5d**; mp 93–95 °C.

**General Procedure for the Synthesis of Semifluorinated Side-Chain Ionenenes.** In a 25 mL flask, 0.34 g (3 mmol) of **3** was dissolved in a solution of 2 mL of absolute ethanol and 1 mL of  $N,N'$ -dimethylformamide, and then 1.943 g (3.5 mmol) of **5b** was added, the air was exchanged with nitrogen, and the reaction was maintained at 70 °C for at least 3 weeks. The polymer was worked up by slow precipitation in diethyl ether and repeatedly washed with warm diethyl ether several times in order to remove unreacted **5b**. A total of 1.69 g of **6b** (yield 84%) was obtained after drying in a vacuum oven at 40 °C overnight.

**Characterization.** Differential scanning calorimeter (DSC) measurements were performed using a DuPont 910 DSC with a DuPont 2000 controller. Five to ten milligram samples were used with heating and cooling rates of 10 and 5 °C/min, respectively.

$^1\text{H}$  and  $^{19}\text{F}$  NMR spectra were obtained on a Varian 200 at 200 MHz for  $^1\text{H}$  and 188.2 MHz for  $^{19}\text{F}$ . The polyamide, polyamine, and fluoro compounds were dissolved in deuterated chloroform and measured at room temperature. For the

semifluorinated alkyl side-chain ionenes, the NMR spectra were measured with a Varian 400 NMR spectrometer at 50 °C in deuterated methanol. Chemical shifts were referenced to TMS for  $^1\text{H}$  and  $^{13}\text{C}$  NMR and to  $\text{CF}_3\text{Cl}$  for  $^{19}\text{F}$  NMR.

Polarizing optical micrographs were recorded using a Nikon microscope with a Mettler FP 80 central processor hotstage and a FX-35DX camera. Melting points, textures, and transition temperatures were detected at a heating rate of 1 °C/min. Infrared spectra were performed on a Mattson 2020 Galaxy Series FTIR with 4  $\text{cm}^{-1}$  resolution using 32 scans. Samples were pressed in a KBr tablet or cast onto a NaCl crystal plate.

Wide-angle X-ray diffraction (WAXD) patterns were obtained by using a SCINTAG  $\theta$ – $\theta$  diffractometer with a Ni-filtered X-ray tube ( $\text{Cu K}\alpha = 1.5418 \text{ \AA}$ ). The tube was operated at 45 kV and 40 mA. Continuous scans were performed at rates of 0.5–1°/min. The temperature-dependent X-ray experiments were performed at the Cornell High Energy Synchrotron Source (CHESS), with an X-ray wavelength of 0.908 Å. The diffraction patterns were recorded with a CCD camera for 5 s at a 92 mm sample-to-detector distance and 5 °C/min heating rate.

X-ray photoelectron spectroscopy (XPS) was performed on a SSL-100-3 photoelectron spectrometer using a monochromatic Al  $\text{K}\alpha$  source (1486.6 eV). Spectra were collected from the 600  $\mu\text{m}^2$  X-ray beam spot on the spin-coated ionene film surface. The fluorine/carbon ratios were calculated from the relative intensity in the C 1s region. Surface segregation of the fluorinated side chain was determined by varying the take-off angle, i.e., the angle between the surface plane and the detector.

Near-edge X-ray absorption fine structure (NEXAFS) analysis was carried out at the National Synchrotron Light Source (NSLS, U7A beamline) in Brookhaven National Laboratory. The electron yield was measured at 90° and 20° incidence angles in order to probe the molecular bond orientations.

Contact angles were determined using a NRC contact angle goniometer Model 100–00 (Ramé-Hart Inc.) at 20 °C. Self-assembling films were prepared by spin-coating a 5% ionene solution in methanol onto a cover glass at room temperature. The contact angles reported were the average of four measurements. The advancing contact angle was read by injecting a 4  $\mu\text{L}$  liquid drop. The receding contact angle was measured by removing about 3  $\mu\text{L}$  of liquid from the drop, and the static contact angle was obtained from a drop of solvent (ca. 4  $\mu\text{L}$ ) on the surface. Linear alkanes and methyl-terminated poly(dimethylsiloxane) oligomers (Gelest Inc.) were used as standards to measure the critical surface tension.<sup>32</sup>

## Results and Discussion

**Synthesis.** The synthesis of  $N$ -alkyl aliphatic polyamides (**2**) has attracted little attention because these materials have a much lower melting point than many commercial polyamides due to a lack of hydrogen bonding<sup>33</sup> between the polymer chains. Interfacial condensation of  $N,N'$ -dimethylhexanediamine with adipoyl chloride at the hexane/water or chloroform/water interface produced only oligomers with very poor (0–15%) yields. The reason is that secondary diamines have limited solubility in water and poor reactivity compared with primary diamines. In contrast, the product polyamide has high solubility in chloroform, which makes it more difficult to attain a high molecular weight polyamide.

To increase the reactivity of  $N,N'$ -dimethylhexanediamine, in contrast to the general synthesis of nylon-6,6 at 200 °C,<sup>29</sup> high temperatures (300 °C) were required to prepare an  $N$ -alkylpolyamide oligomer for subsequent polycondensation. The final step in eliminating water was carried out below 250 °C to prevent degradation. The  $^1\text{H}$  NMR spectrum of poly( $N,N'$ -dimethylhexamethylene adipamide) is shown in Figure 1a, and the assignments are listed in the Experimental Section. Due to stereochemical effects, the protons on the  $\text{N}-\text{CH}_3$

groups split into two equivalent peaks at 2.87 and 2.94 ppm. From end-group analysis, the degree of polymerization was estimated to be ca. 30–40. From DSC measurements, the glass transition temperature of **2** is  $-1\text{ }^{\circ}\text{C}$ , and the melting point at  $72\text{ }^{\circ}\text{C}$  is similar to that given in the literature.<sup>34</sup>

Homogeneous reduction of the polyamide to the polyamine is highly efficient because of the good solubility of the polyamide **2** in normal organic solvents. The reduction of **2** using borane/dimethyl sulfide in THF at  $50\text{ }^{\circ}\text{C}$  is quantitative without detectable degradation. From FTIR spectra, the carbonyl groups ( $1631\text{ cm}^{-1}$ ) were entirely converted to methylene groups as confirmed by the  $^1\text{H}$  NMR spectrum of poly(*N*-methyl-1,6-hexaneamine) (**3**) given in Figure 1b. The small peaks at 2.38 and 2.56 ppm are *N*-methylamine end groups. In contrast to the heterogeneous reduction of poly-(hexamethyleneimine),<sup>35</sup> the molecular weight of which decreases on average three to four times, no detectable molecular weight decrease was observed in this reaction after homogeneous reduction by end-group analysis. The resultant poly(*N*-methylhexaneamine) (**3**) is a crystalline polymer exhibiting a melting point just below room temperature. The glass transition of **3** is  $-74\text{ }^{\circ}\text{C}$ ; the melting point is  $14\text{ }^{\circ}\text{C}$  with a melting enthalpy of  $2.16\text{ kJ/mol}$ .

The resulting  $\omega$ -perfluoroalkylalkanols are the same as those reported by Höpken et al.<sup>31</sup> The bromination reaction of **3** runs smoothly using 50–100% excess carbon tetrabromide and triphenylphosphine at  $-5$  to  $10\text{ }^{\circ}\text{C}$ . The conversion of hydroxide to bromide is complete after 6–8 h as monitored by  $^1\text{H}$  (Figure 1c) and  $^{19}\text{F}$  NMR. If the reaction temperature is increased to  $40\text{ }^{\circ}\text{C}$ , the maximum conversion of the alkanol to bromide can only reach about 80%. The triphenylphosphine oxide and products were readily separated by using a short silica column with diethyl ether as the elution solvent, and high-purity  $\omega$ -perfluoroalkyl bromide was obtained by distillation or sublimation.

The attachment reaction of the semifluorinated 1-bromoalkanes (**5**) with the polyamine backbone (**3**) depends strongly on the length of the methylene spacer of the perfluoroalkyl groups. Direct reaction of **5a** or perfluoroalkyl iodide with the polyamine will not produce the fluorinated side-chain ionenes. While the reaction proceeded, the polyamine solution became dark brown and the FTIR spectra of the products indicated that only a tiny amount of  $\text{CF}_2$  ( $1100\text{--}1200\text{ cm}^{-1}$ ) was present in the polymer.  $^1\text{H}$  and  $^{19}\text{F}$  NMR showed that a large portion of the amine groups were neutralized by hydroiodic acid or hydrobromic acid (detected by  $\text{AgNO}_3$ ) but no fluorocarbon chains were attached. This indicates that  $\alpha$ - or  $\beta$ -hydrogen elimination reaction induced by strong C–F groups dominates the expected Menshutkin reaction. **5b–f** were reacted with the polyamine to form the semifluorinated alkyl side-chain ionenes in good yield. To overcome the low reactivity of the polyamine, high concentrations, an aprotic polar solvent, and a high reaction temperature were used to achieve high quaternization yields.<sup>36</sup> As determined from  $^1\text{H}$  NMR spectra (Figure 1d), more than 80% of the amine groups were converted to quarternary ammonium groups after more than 3 weeks of reaction in absolute ethanol/DMF (2/1) at  $65\text{ }^{\circ}\text{C}$ . However, it seems difficult to achieve higher conversions (more than 90%) by increasing the temperature and prolonging the reaction time. The quarternary ammonium group resonances at 3.4 and 3.1 ppm and the  $\text{CF}_2\text{CH}_2$  groups at 2.02 ppm

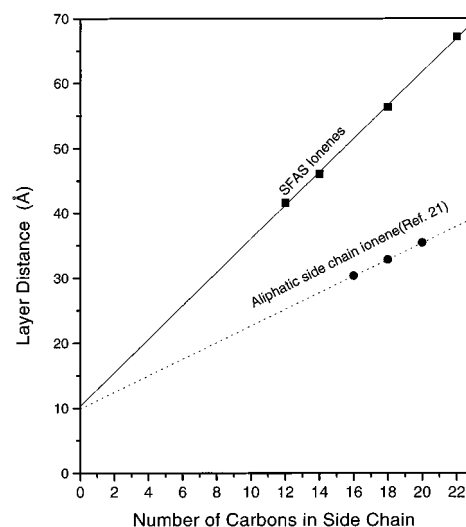


**Figure 2.** Layer distance of alkyl and semifluorinated alkyl side-chain ionenes.

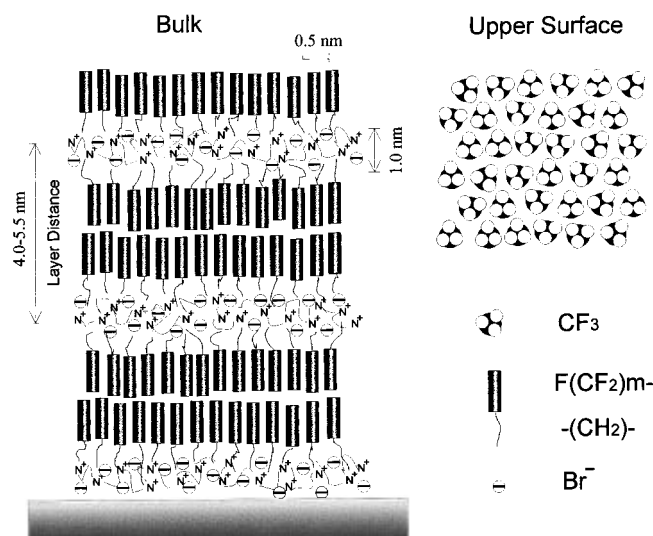
**Table 1.** X-ray Diffraction Results of Semifluorinated Alkyl Side-Chain Ionen

| name               | state  | d space (Å)                  |
|--------------------|--------|------------------------------|
| I-6,6-F8H4,Me/Br   | film   | 42.0, 20.7, 13.9, 10.43      |
|                    | powder | 38.3, 19.1, 12.78, 5.04      |
| I-6,6-F8H6,Me/Br   | film   | 45.5, 23.2, 15.5, 11.41      |
|                    | powder | 42.2, 28.5, 21.3, 14.3, 5.08 |
| I-6,6-F8H10,Me/Br  | film   | 56.0, 27.9, 18.8, 14.2       |
|                    | powder | 55.3, 33.1, 27.5, 16.6, 5.06 |
| I-6,6-F12H10,Me/Br | film   | 67.0, 33.4, 22.5, 16.9       |
|                    | powder | 65.6, 32.5, 21.6, 4.91       |

confirmed the expected ionenes. The assignments for  $^{13}\text{C}$  NMR spectra of SFAI **6b** (I-6,6/Me-F8,H4/Br) at  $50\text{ }^{\circ}\text{C}$  in methanol are listed in the Experimental Section. From the  $^{13}\text{C}$  NMR spectra, the unreacted amine can also be identified. The FTIR spectra showed very strong  $\text{CF}_2$  stretching bands between  $1100$  and  $1200\text{ cm}^{-1}$ . The attachment reaction results are listed in Table 1. From the weight increase and the data from the  $^1\text{H}$  NMR spectra, we estimate the yield to be around 85%.

**Solid-State Properties of Semifluorinated Side-Chain Ionen.** The semifluorinated side-chain ionenes are waxlike white solids at room temperature. They are soluble in hot methanol, ethanol, and DMF but insoluble in nonpolar solvents such as toluene and heptane. Solubility decreases significantly with increasing the number of fluorocarbon units. Ionene **6f** (I-6,6-F12H10,Me/Br), for example, is almost insoluble in hot methanol.

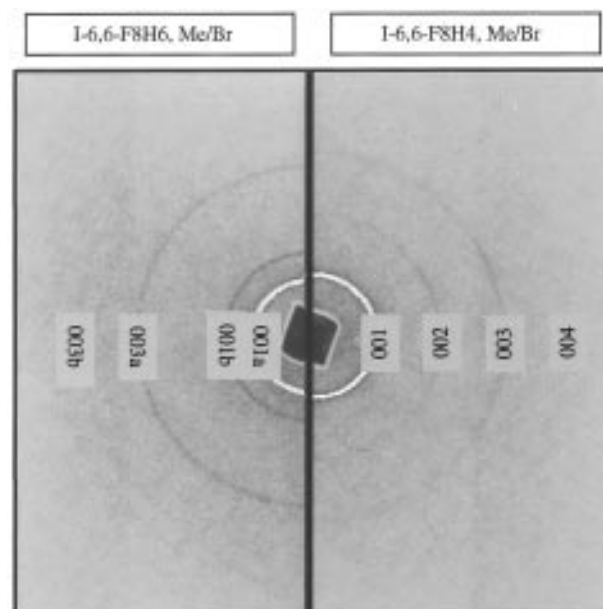
X-ray diffraction results are listed in Table 1. All side-chain ionenes have one wide-angle ring with a d-spacing of  $4.9\text{--}5.1\text{ Å}$ , which arises from the intersegment spacing of the perfluorocarbon units. At small angles, X-ray diffraction of the ionenes exhibited a highly organized layer structure (Figure 3) in which the second, third, and fourth orders can be detected. For solution-cast films, dependence of the layer distance and the number of side-chain carbons is plotted in Figure 2. For comparison, the relationship between layer distance and carbon number of long aliphatic side-group ionenes was also plotted. In the plot, all of the semifluorinated alkyl side-chain ionenes have a layer distance of ca.  $10\text{--}20\text{ Å}$  larger than those of the aliphatic side-chain ionenes. Extrapolating to the number of carbons per side chain equal to zero reveals the same layer distance, indicating that the charged layer from both types of side-chain ionenes is around the same

**Chart 1. Schematic Structure of Self-Assembling Films of Semifluorinated Side-Chain Ionenes**

thickness of 10 Å. The slope of the semifluorinated side-chain ionenes is 2.5 Å per CH<sub>2</sub>, which is exactly double that of the aliphatic side-chain ionenes. Since the aliphatic side-chain ionene forms an interdigitated bilayer structure,<sup>19</sup> bond-length estimation of the semifluorinated side-chain ionene, in this case, leads to the conclusion that a head-to-head bilayer structure is formed. Because the diffraction peaks from the ionic groups are absent, one can conclude that the ionene main-chain charged layer was randomly organized. In order to understand the observed X-ray diffraction results of SFASI, a structural model is presented in Chart 1. Here the rigid-rod perfluorocarbon segments connected to the flexible hydrocarbon spacers are hexagonally packed into the main-chain charged layer. The difference in packing between the aliphatic and semifluorinated side-chain ionenes might be explained by the difference in cross-sectional area of the side groups. As reported previously, the cross-sectional area per CF<sub>2</sub> group is 28.3 Å<sup>2</sup>, but for CH<sub>2</sub> groups it is only 18.6 Å<sup>2</sup>. If the two types of ionenes (aliphatic and semifluorinated side chain) have the same charge density and side-chain density, interdigitated packing of the fluorocarbon side chain would require much more space than is available since the ionic layer structure is the same as that for the aliphatic side-chain ionene.

The side-chain layer packing is strongly dependent on the side-chain structure and sample treatment. Powdered ionene samples obtained from either solution precipitation or nonequilibrium processing showed more complex and ordered side-chain packing than the solution-cast films. The small-angle X-ray diffraction patterns of **6b** (I-6,6-F8H4,Me/Br) and **6c** (I-6,6-F8H6,Me/Br) are presented in Figure 3, where **6b** side chains have a regular layer packing with a *d* spacing of 38.4 Å, about 3 Å smaller than that of the film sample. However, **6c** has two kinds of layered structures with *d* spacings at 42.2 and 28.5 Å. The 28.5 Å layer spacing is that of an interdigitated side chain. Thus, the **6c** powder sample forms both interdigitated and head-to-head structures. Similarly, the **6d** powder pattern also possesses two kinds of layered structures with *d* spacings of 55.3 and 33.1 Å.

DSC curves showed a melting transition for -CF<sub>2</sub>- groups at a temperature close to the transition of the parent semifluorinated 1-bromoalkanes (Table 2). How-

**Figure 3.** Small-angle X-ray diffraction of ionenes.**Table 2. Thermal Transitions of Semifluorinated Alkyl Bromide and Corresponding Side-Chain Ionene**

| sample             | <i>T<sub>m</sub></i><br>(°C) | Δ <i>H<sub>m</sub></i><br>(kJ/mol) | <i>T<sub>mc</sub></i> <sup>a</sup><br>(°C) | <i>T<sub>d</sub></i><br>(°C) |
|--------------------|------------------------------|------------------------------------|--|------------------------------|
| F8H4Br             | 34.8                         | 20.8                               |  |                              |
| I-6,6-Me,F8H4/Br   | 45.1                         | 1.4                                | 233  | 243                          |
| F8H6Br             | 38.5                         | 27.6                               |  |                              |
| I-6,6-Me,F8H6/Br   | 47.2                         | 1.3                                | 237  | 248                          |
| F8H10Br            | 44.0                         | 38.5                               |  |                              |
| I-6,6-Me,F8H10/Br  | 50.1                         | 1.6                                | 232  | 276                          |
| F10H10Br           | 70.7                         | 32.3                               |  |                              |
| I-6,6-Me,F10H10/Br | 56.0, 76.3                   | 3.4 <sup>b</sup>                   | 241  | 279                          |
| F12H10Br           | 80.1, 96.5                   | 8.9, 21.9                          |  |                              |
| I-6,6-Me,F12H10/Br | 79.2, 102                    | 5.7 <sup>b</sup>                   | 238  | 272                          |

<sup>a</sup> The clearing transition temperature was observed with a polarizing optical microscope with heating at 5 °C/min. <sup>b</sup> Total transition enthalpy.

ever, the transition entropy is much lower because the aliphatic spacer groups are disordered. This transition is attributed to melting of the semifluorinated alkyl side chain as confirmed from the WAXD experiments at a temperature just above the transition. For example, the diffraction peaks of **6b** at wide angles (5.0 Å) disappeared after the temperature was increased to 60 °C (transition temperature is 45 °C). Fluorinated side-chain ionenes displayed strong birefringence under a polarizing light microscope. The birefringence disappeared only above the main-chain softening temperature. Upon cooling, semifluorinated ionenes displayed smectic fan-shape textures as do aliphatic side-chain ionenes (Figure 4). From the X-ray diffraction studies and DSC measurements, the packing of the semifluorinated side-chain ionenes can be identified as a smectic-like layer structure as illustrated in Chart 1.

For the long semifluorinated side-chain ionene **6e**, two transitions (Figure 5) were detected from the DSC trace. For a long aliphatic side-chain ionene,<sup>19</sup> similar transitions were observed, and the low-temperature transition was attributed to a crystalline-to-rotator phase transition. For the semifluorinated alkyl side chain, the first transition was probably a high-order smectic to low-order smectic phase transition. Thermal stability not only depends on the counterions similar to "normal" ionenes (BF<sub>4</sub><sup>-</sup> counterions are much more stable than Br<sup>-</sup> counterions) but also depends on the length of the



**Figure 4.** Smectic fan-shaped texture of I-6,6-F8H4,Me/Br at 493 K as observed by polarizing optical microscopy.

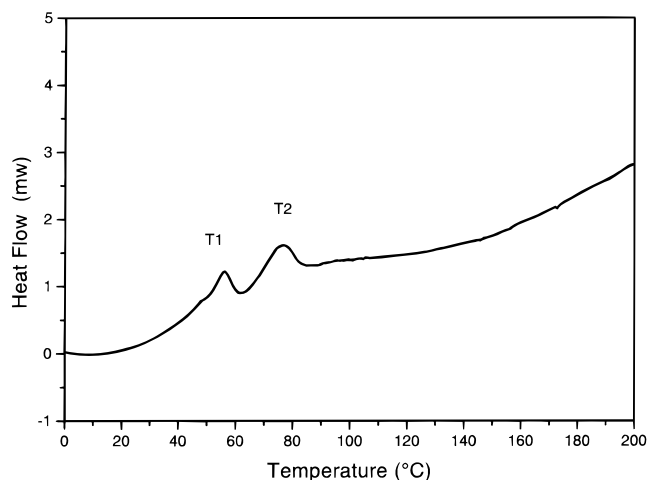


**Figure 5.** DSC thermogram of semifluorinated side-chain ionene (I-6,6-F10H10,Me/Br).

spacer groups. The onset decomposition temperature is increased as the methylene spacer length increased from 4 to 10 carbon atoms (Table 2).

Fluorinated side-chain ionenes displayed strong birefringence under a polarizing light microscope. The birefringence disappeared only above the main-chain melting temperature. Upon cooling, ionenes displayed smectic textures as did aliphatic side-chain ionenes.

**Surface Behavior of Semifluorinated Alkyl Side-Chain Ionene.** The goal of this study was to explore the possibility of self-assembly of mesogenic semifluorinated side-chain ionenes at a film surface and especially the surface arrangement of low surface energy

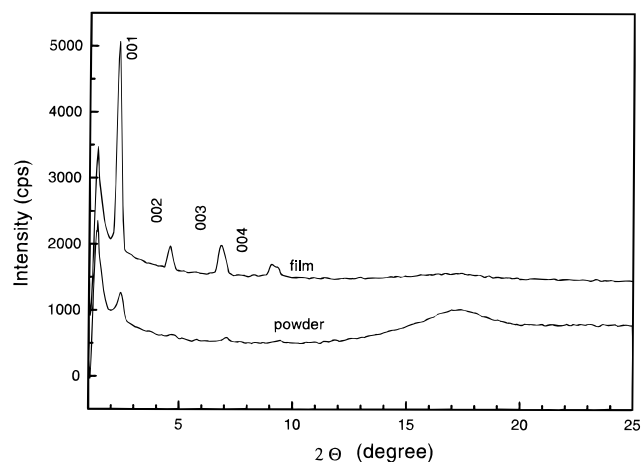


**Figure 6.** X-ray diffraction patterns of semifluorinated side-chain ionene (I-6,6-F8H4,Me/Br) powder and film.

**Table 3. List of Contact Angles of Different Solvents on a Semifluorinated Alkyl Side-Chain Ionene (I-6,6-F8H4,Me/Br) Film Surface at 20 °C**

| solvent             | surface tension (dyn/cm) | stationary angle (deg) <sup>b</sup> | advancing angle (deg) <sup>b</sup> | receding angle (deg) <sup>b</sup> | average angle (deg) <sup>b</sup> |
|---------------------|--------------------------|-------------------------------------|------------------------------------|-----------------------------------|----------------------------------|
| PDMS 1 <sup>a</sup> | 15.9                     | 43                                  |                                    |                                   | 43                               |
| PDMS 2              | 17.4                     | 51                                  | 54                                 | 45                                | 50                               |
| PDMS 3              | 18.7                     | 55                                  | 60                                 | 51                                | 55.3                             |
| PDMS 4              | 20.1                     | 59                                  | 62                                 | 53                                | 58                               |
| hexane              | 18.4                     | 56                                  |                                    |                                   | 56                               |
| octane              | 21.8                     | 60                                  | 68                                 | 57                                | 62                               |
| decane              | 23.9                     | 66                                  | 62                                 | 71                                | 66.5                             |
| dodecane            | 25.4                     | 70                                  | 65                                 | 76                                | 70.8                             |
| tetradecane         | 26.7                     | 73                                  | 79                                 | 69                                | 74                               |
| hexadecane          | 27.4                     | 75                                  | 81                                 | 69                                | 75                               |
| water               | 71.4                     | 114                                 | 121                                | 111                               | 116                              |

<sup>a</sup> Commercial product of poly(dimethylsiloxane) oligomers (trimethylsiloxy terminated) from Gelest Inc. <sup>b</sup> Error of measurement ca.  $\pm 1^\circ$ .

trifluoromethyl end groups. X-ray diffraction revealed that well-oriented side-chain ionene layer structures were formed on a silicon surface. As illustrated in Figure 6, the X-ray diffraction pattern of the thin films showed a much stronger intensity in the small-angle region and a lower intensity at wide angles as compared to powdered ionene samples.

From this structural analysis, ionenes with head-to-head antiparallel packing may be expected to expose  $\text{CF}_3$  end groups at the surface due to their low surface energy. Surface tension as measured from contact angles is the simplest approach to assess the surface composition. The contact angle measurements on a spin-coated **6b** (I-6,6-F8H4,Me/Br) film is shown in Table 3. The fluorinated alkyl side-chain ionenes have a very large advancing water contact angle ( $121^\circ$ ) which is even larger than poly(tetrafluoroethylene) ( $115^\circ$ ) under the same conditions. Using a series of solvents of known surface tension to measure the contact angle ( $\theta$ ) and plotting  $\cos(\theta)$  versus surface tension is known as a Zisman plot. For measuring the critical surface tension of the low-energy surface, we chose a family of low surface tension poly(dimethylsiloxane) oligomers and alkanes as standards, the contact angles of which are also listed in Table 3. Extrapolating the contact angle  $\theta$  to zero (i.e.,  $\cos \theta = 1$ ) reveals a critical surface tension for I-6,6-F8H4,Me/Br to be 8.0 dyn/cm (Figure 7). This is close to that of a uniform  $-\text{CF}_3$  surface as determined from LB monolayers of perfluoroalkylcarboxylic acids. That means the hydrophobic  $-\text{CF}_3$  groups

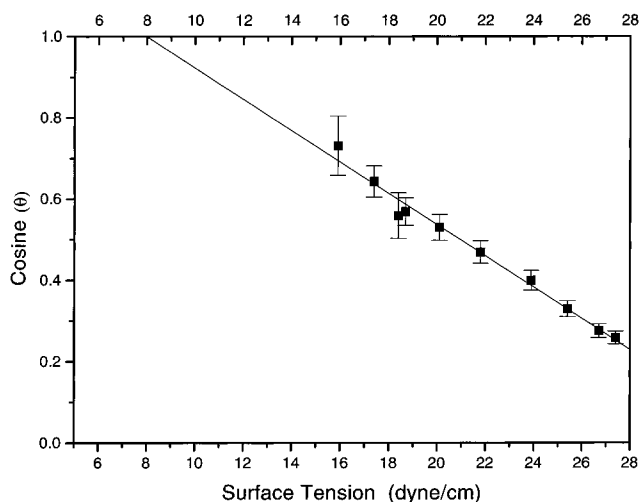


**Figure 7.** Critical surface tension of semifluorinated side-chain ionene (I-6,6-F8H4,Me/Br).

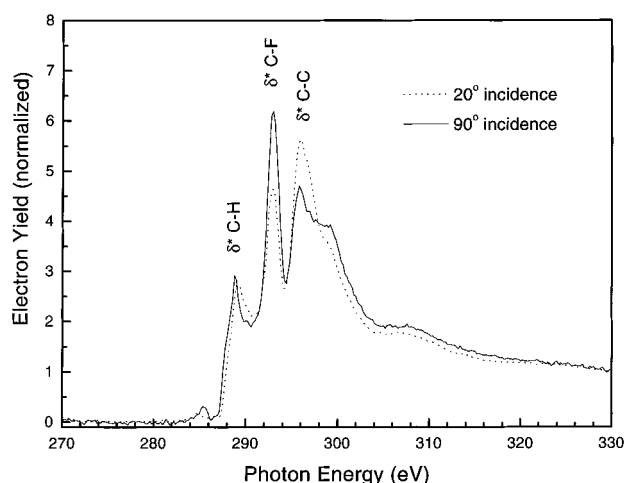


**Figure 8.** NEXAFS spectra of semifluorinated ionene (I-6,6-F8H8,Me/Br) at carbon edge.

are well aligned on the surface and the strong hydrophilic main chain (quaternary ammonium group) is almost completely covered by low surface energy side chains. However, the contact angle–time dependence results showed clear evidence of surface reconstruction; i.e., the contact angle decreased rapidly after 20 min of contact with water. This reconstruction process may be attributed to the unreacted polyamine behaving as a structural defect point, which enables the hydrophilic backbone to be brought to the surface.<sup>3,4</sup>

The surface structure of the ionenes was further characterized by XPS and NEXAFS analysis. Upon comparison with XPS measurement at the normal take-off angle, a higher C–F bond concentration was detected at 20°. These angle-dependent XPS results indicated that fluorinated side groups enriched the polymer film surface. The orientation of the semifluorinated side chain in the top 3 nm was examined by polarization-dependent NEXAFS at Brookhaven National Laboratory.<sup>37</sup> In Figure 8, the carbon region NEXAFS spectra were normalized at 330 eV for comparison of the carbon species. The fluorocarbon groups were preferentially oriented at the air–film surface. This can be demonstrated because the stronger electronic yield intensity of the  $\delta^*$  C–F bond at 293 eV was observed with normal X-ray incidence angle where the electric vector is parallel to the surface direction as well as the C–F bond polarization direction. In contrast, the average polar-

ization of  $\delta^*$  C–C bonding in the vertical direction of the C–F bond has the reverse intensity dependence.

## Conclusion

The results from the synthesis and characterization of new semifluorinated side-chain ionenes demonstrate that the self-assembly process at a film surface could be tailored by the introduction of semifluorinated liquid-crystal groups. In this structure, surface alignment is generated by reducing the surface energy of the system, i.e., surface organization of low surface energy –CF<sub>3</sub> groups. Compared with semifluorinated side-chain block copolymers reported elsewhere,<sup>27</sup> although both polymer families possess extremely low surface energies, the semifluorinated ionene surface is much less stable than that of the block copolymer. As indicated by DSC results, the transition enthalpy of a given semifluorinated side chain in ionene polymers (1–3 kJ/mol) is much smaller than that of the corresponding block copolymer (3–12 kJ/mol). Therefore, the fluorinated side group of the block copolymer possessed a higher level of organization, an observation which is in agreement with the smaller *d* spacing of the wide-angle X-ray diffraction peak due to the spacing between fluorocarbon groups.

Another factor related to the surface reconstruction of ionenes is the strong interaction between the ammonium group with water. Being efficient surfactants, the small-molecule fluorinated surfactants are commercially available and extensively used. As a macromolecular cationic surfactant, semifluorinated side-chain ionenes may exhibit superior surface-active properties eventually to be used as ionic conducting films for electrochemical applications or function in the biomedical area as fluorinated surfactants.

In summary, a family of semifluorinated alkyl side-chain ionenes (SFASI) has been synthesized by reaction of semifluorinated alkyl bromides (SFAB) with poly(*N,N'*-dimethyl-1,6-hexanediamine), which was prepared by reduction of poly(*N,N'*-dimethylhexamethyleadipamide). In a solid-state film, the perfluorocarbon units tend to self-organize into a hexagonal array and form a head-to-head organization between charged layers. The surface energy of a SFASI polymer, as estimated from critical surface tension, was 8 dyn/cm at 20 °C using Zisman's method. This value is smaller than that of poly(tetrafluoroethylene), which also indicates that the CF<sub>3</sub> end groups in the perfluorocarbon segments tend to align at the surface when the SFASI film is spin coated from a polymer solution in methanol. NEXAFS and XPS measurements confirm this picture in the as-cast and annealed states. However, reconstruction of the surface molecules was observed in polar environments and is believed to be mainly due to structural defects in the backbone.

**Acknowledgment.** This research was supported by the Office of Naval Research (Grant No. N00014-92-J-1246) and National Science Foundation. Valuable discussions with Prof. E. J. Kramer are gratefully acknowledged. We acknowledge the Material Science Center (MSC), Cornell High Energy Synchrotron Source (CHESS), and National Synchrotron Light Source (NSLS) at Brookhaven National Laboratory (BNL) for use of their facilities. Dr. B. M. DeKoven (Dow Chemical Corp.) and Dr. D. A. Fisher (BNL) are also thanked for their assistance with NEXAFS measurements.

## References and Notes

- (1) Kobayashi, H.; Owen, M. J. *Trends Polym. Sci.* **1995**, 3 (10), 330.
- (2) Schmidt, D. L.; Coburn, C. E.; Dekoven, B. M.; Potter, G. E.; Meyers, G. F.; Fisher, D. A. *Nature* **1994**, 368, 39–41.
- (3) Chapman, T. M.; Benrashid, R.; Marra, K. G.; Keener, J. P. *Macromolecules* **1995**, 28, 331–335.
- (4) Chapman, T. M.; Marra, K. G. *Macromolecules* **1995**, 28, 2081–2085.
- (5) Lenk, T. L.; Hallmark, V. M.; Hoffmann, C. L.; Rabolt, J. F.; Castner, D. G.; Erdelen, C.; Ringsdorf, H. *Langmuir* **1994**, 10, 4610.
- (6) Hwang, S. S.; Ober, C. K.; Perutz, S.; Iyengar, D.; Schneggenburger, L. A.; Kramer, E. J. *Polymer* **1995**, 36, 1321.
- (7) Owen, M. J. *J. Coat. Technol.* **1981**, 53 (679), 49–53.
- (8) Lindner, E. *Biofouling* **1992**, 6, 193.
- (9) Pfeifer, C. R. U.S. Patent 4861501A, 1989.
- (10) Wu, S. H. *Polymer Interfaces and Adhesion*; Marcel Dekker: New York, 1982.
- (11) Lau, W. Y.; Burns, C. M. *J. Polym. Sci., Polym. Phys. Ed.* **1974**, 12, 431.
- (12) Bernett, M. K.; Zisman, W. A. *J. Phys. Chem.* **1960**, 64, 1292.
- (13) Dettre, R. H.; Johnson, R. E., Jr. *J. Colloid Interface Sci.* **1966**, 21, 367.
- (14) Dettre, R. H.; Johnson, R. E., Jr. *J. Colloid Interface Sci.* **1969**, 31, 568.
- (15) Fox, H. W.; Zisman, W. A. *J. Colloid Sci.* **1950**, 5, 514.
- (16) Suzuki, M.; Saotome, Y.; Yanagisawa, M. *Thin Solid Films* **1988**, 160, 453.
- (17) Nakahama, H.; Miyato, S.; Wang, T.; Tasaka, S. *Thin Solid Films* **1986**, 141, 165.
- (18) Meyer, W. H.; Wang, J. G.; Wegner, G. *Polym. Prepr. (Am. Chem. Soc., Div. Polym. Chem.)* **1995**, 36 (1), 558.
- (19) Wang, J. G.; Meyer, W. H.; Wegner, G. *Acta Polym.* **1995**, 46, 233.
- (20) George, L. G., Jr. *Langmuir* **1991**, 7, 3054.
- (21) Li, M. Y.; Acero, A. A.; Huang, Z. Q.; Rice, S. A. *Nature* **1994**, 367, 151.
- (22) Thomas, E. L.; Anderson, D. M.; Henkee, C. S.; Hoffman, D. *Nature* **1988**, 334, 598.
- (23) Bates, F. S. *Annu. Rev. Phys. Chem.*, **1990**, 41, 525.
- (24) Bedford, R. G.; Dunlap, R. D. *J. Am. Chem. Soc.* **1958**, 80, 282.
- (25) Shull, K. R.; Kramer, E. J.; Hadziioannou, G.; Tang, W. *Macromolecules* **1990**, 23, 4780.
- (26) Iyengar, D. R.; Perutz, S. M.; Dai, C.-A.; Ober, C. K.; Kramer, E. J. *Macromolecules* **1996**, 29, 1229.
- (27) Wang, J. G.; Mao, G. P.; Ober, C. K.; Kramer, E. J. *Macromolecules* **1997**, 30, 1906.
- (28) Rembaum, A.; Noguchi, H. *Macromolecules* **1972**, 5, 261.
- (29) Antonietti, M.; Henke, S.; Thünemann, A. *Adv. Mater.* **1996**, 8, 41.
- (30) Hill, R.; Walker, E. E. *J. Polym. Sci.* **1948**, 3, 609.
- (31) Höpken, J.; Möller, M.; Boileau, S. *New Polym. Mater.* **1991**, 2, 339.
- (32) Zisman, W. A. *Contact angle, wettability, and adhesion*; American Chemical Society: Washington, DC, 1964.
- (33) Baker, W. O.; Fuller, C. S. *J. Am. Chem. Soc.* **1943**, 65, 1120.
- (34) Korshak, V. V.; Frunze, T. M. *Synthetic Hetero-Chain Polyamides*; Daniel Davey & Co. Inc.: New York, 1964.
- (35) Perner, T.; Schulz, R. C. *Br. Polym. J.* **1987**, 19, 181.
- (36) Wang, J.-G.; Meyer, W. H.; Wegner, G. *Macromol. Chem. Phys.* **1994**, 194, 1775.
- (37) Schmidt, D. L.; Dekoven, B. M.; Coburn, C. E.; Potter, G. E.; Meyers, G. F.; Fisher, D. A. *Langmuir* **1996**, 12, 518.

MA9700901